ENT Updates
https://ojs.ukscip.com/index.php/ENTU

Review

Shear Wave Elastography: A New Frontier in Head and Neck Imaging

Sivan Sathish [1,*], Ankita Jain [2], Vaishali Malik [1] and Vikas Singh [2]

[1] Department of Oral Medicine and Radiology, Teerthanker Mahaveer Dental College and Research Centre, Teerthanker Mahaveer University, Moradabad 244001, India

[2] Department of Public Health Dentistry, Teerthanker Mahaveer Dental College and Research Centre, Teerthanker Mahaveer University, Moradabad 244001, India

[*] Correspondence: sivansathishmfds@yahoo.co.in

Received: 1 May 2026; **Revised:** 3 June 2026; **Accepted:** 9 June 2026; **Published:** 10 June 2026

Abstract: Shear Wave Elastography (SWE) has emerged as a transformative ultrasound-based imaging modality for the quantitative assessment of tissue stiffness, providing valuable insights into the biomechanical properties of normal and diseased tissues. Unlike conventional ultrasonography, which primarily relies on morphological evaluation, SWE enables real-time, reproducible, and relatively operator-independent measurements of tissue elasticity. In recent years, its application has expanded considerably within head and neck imaging, where tissue stiffness serves as a potential biomarker for disease characterization, diagnosis, and treatment monitoring. This narrative review provides a comprehensive overview of the physical principles, quantitative parameters, technical considerations, and clinical applications of SWE in the head and neck region. Current evidence supporting its use in thyroid nodules, salivary gland disorders, cervical lymph node evaluation, oral soft tissue lesions, periodontal assessment, and temporomandibular joint and masticatory muscle disorders is discussed. The integration of SWE with conventional B-mode and Doppler ultrasonography has demonstrated improved diagnostic confidence, enhanced lesion characterization, and reduced reliance on invasive diagnostic procedures in selected clinical scenarios. Despite its promising clinical utility, several challenges remain, including variability in acquisition protocols, machine-dependent elasticity measurements, lack of universally accepted cutoff values, and limited standardization across institutions. Nevertheless, ongoing technological advancements and the growing interest in artificial intelligence, radiomics, and multiparametric ultrasound approaches are expected to further enhance the diagnostic and prognostic capabilities of SWE. Overall, SWE represents a valuable non-invasive adjunct to routine head and neck imaging and holds significant potential as a quantitative biomarker in precision medicine.

Keywords: Elastography; Head and Neck Imaging; Quantitative Ultrasound; Shear Wave Elastography; Tissue Stiffness

1. Introduction

The field of head and neck imaging is undergoing a technological and perspective shift from predominantly qualitative interpretation toward quantitative, reproducible, and biologically meaningful imaging biomarkers [1,2]. Traditional imaging evaluation has largely relied on morphological descriptors such as lesion size, shape, margins, internal architecture, and enhancement characteristics. Although these features remain clinically indispensable, they are inherently subjective and susceptible to interobserver variability [3]. Moreover, morphological assessment

often reflects late structural alterations rather than early microenvironmental changes. In an era increasingly driven by precision medicine, risk stratification algorithms, and outcome prediction models, there is a growing demand for non-invasive imaging techniques that provide objective metrics reflecting tissue biology rather than solely anatomy. Among the various biological properties that can be exploited for imaging, mechanical characteristics of tissue have emerged as particularly informative. The stiffness of a tissue is not arbitrary, it is determined by its cellular density, extracellular matrix composition, collagen content, vascular architecture, and interstitial pressure [4]. Pathological processes induce predictable alterations in these biomechanical properties. Malignant tumors frequently demonstrate increased stiffness due to hypercellularity, desmoplastic stromal reaction, extracellular matrix remodeling, and elevated interstitial pressure. In contrast, cystic degeneration or necrosis reduces stiffness, while chronic inflammation and fibrosis often produce diffuse parenchymal stiffening. Therefore, tissue stiffness represents a measurable surrogate of underlying histopathology and microenvironmental remodeling. Elastography was developed as an imaging technique to quantify these mechanical properties in vivo [5,6]. Conceptually analogous to clinical palpation, elastography translates the subjective perception of firmness into objective imaging data. However, unlike manual palpation, elastographic techniques generate reproducible, image-based maps and numerical parameters that allow quantitative assessment [7]. By measuring tissue response to mechanical stress, elastography provides insights into biomechanical alterations that are not apparent on conventional structural imaging. The need for such a technique becomes evident when examining the limitations of established imaging modalities in head and neck practice. B-mode ultrasonography remains the first-line modality for evaluating thyroid nodules, salivary gland masses, and cervical lymphadenopathy [8–10]. While it offers high spatial resolution and real-time assessment, its interpretation is predominantly morphology-based. Features such as hypoechogenicity, irregular margins, microcalcifications, and absence of nodal hilum improve diagnostic suspicion but lack absolute specificity. Benign hyperplastic nodules, inflammatory conditions, and low-grade malignancies frequently demonstrate overlapping grayscale characteristics, leading to indeterminate assessments and potentially unnecessary biopsies [11,12]. Computed tomography provides excellent delineation of deep neck spaces and osseous structures but offers limited soft tissue characterization for subtle parenchymal differences. It does not interrogate tissue biomechanics and involves ionizing radiation exposure [13]. Magnetic resonance imaging provides superior soft tissue contrast and functional sequences such as diffusion-weighted imaging, which indirectly reflect cellular density. Nevertheless, MRI is resource-intensive, less accessible in many settings, and does not routinely provide direct quantitative measures of tissue stiffness [14]. Although MR elastography exists, it remains technically demanding and is not widely integrated into standard head and neck imaging protocols. These limitations highlight a critical unmet need for an imaging approach that is non-invasive, quantitative, reproducible, cost-effective, and capable of reflecting tissue biomechanics in real time. Elastography has evolved to address this gap by enabling non-invasive quantification of tissue biomechanics within routine ultrasound examinations. In particular, shear wave elastography has gained increasing clinical attention owing to its quantitative and reproducible nature. This review aims to analyze the physical principles underlying shear wave elastography, its clinical applications in head and neck pathology, technical limitations, and explore future directions like integration with multiparametric imaging and computational analytics.

2. Materials and Methods

The current review aimed at providing an in-depth analysis of the principles, metrics, and clinical applications of shear wave elastography imaging in the head and neck region. A comprehensive literature search was conducted using major electronic databases, including PubMed, Scopus, Web of Science, and Google Scholar, for articles published between January 2006 and January 2026. The search strategy incorporated both Medical Subject Headings (MeSH) and free-text keywords. Key search terms included “shear wave elastography,” “elastography,” “head and neck imaging,” “quantitative ultrasound,” “tissue stiffness,” “ultrasound elastography,” “thyroid elastography,” “salivary gland elastography,” “cervical lymph node elastography,” “oral lesions elastography,” and “temporomandibular joint elastography.” These terms were combined using Boolean operators (AND/OR) to optimize search sensitivity and specificity. Additional targeted searches were performed using combinations such as “shear wave elastography AND thyroid nodules,” “shear wave elastography AND salivary gland disease,” “shear wave elastography AND lymphadenopathy,” “shear wave elastography AND oral cavity,” and “shear wave elastography AND temporomandibular joint.”

A total of 511 records were initially identified through database searching. After removal of duplicate and clearly irrelevant records, 128 articles underwent title and abstract screening. Subsequently, 47 articles were assessed in full text for eligibility. Following application of the inclusion and exclusion criteria, 34 studies specifically addressing the principles, quantitative assessment, and clinical applications of shear wave elastography in the head and neck region were included in the final narrative synthesis. Screening and selection of studies were performed independently by two reviewers, and any disagreements were resolved through discussion and consensus. Inclusion criteria comprised original research articles, systematic reviews, meta-analyses, and clinically relevant observational studies addressing the technical principles, quantitative assessment, and clinical applications of shear wave elastography in the head and neck region. Preference was given to English-language publications involving human subjects. Studies lacking relevance to head and neck applications, those without quantitative elastographic assessment, and studies with insufficient methodological detail were excluded. Reference lists of selected studies were also manually searched to identify additional relevant publications. As this study was designed as a narrative review rather than a systematic review, a formal risk-of-bias or quality assessment tool was not applied. Instead, studies were prioritized based on methodological quality, clinical relevance, sample size, recency of publication, and overall contribution to the understanding of shear wave elastography applications in head and neck imaging. Recent studies and higher levels of evidence were emphasized to ensure that the synthesized literature remained current and clinically relevant. The collected information was analyzed qualitatively and organized into thematic sections according to anatomical site and clinical application.

3. Principles and Evolution of Elastography

Elastography encompasses a family of ultrasound-based techniques designed to characterize tissue mechanical properties by measuring deformation in response to applied stress [15,16]. The conceptual foundation is derived from biomechanics: when a force is applied to biological tissue, the extent of deformation depends on its intrinsic elastic modulus. Soft tissues deform more readily, whereas stiff tissues resist deformation. Elastographic imaging quantifies this mechanical behavior and integrates it with conventional B-mode imaging, displaying relative or absolute stiffness maps that complement morphological assessment [16]. Ultrasound elastography can be broadly categorized into two major types: strain elastography and shear wave elastography.

3.1. Strain Elastography

Strain elastography represents the earliest widely adopted form of ultrasound elastography. It operates on the principle that tissue deformation, or strain, occurs when external compression is applied. In clinical practice, this compression may be generated manually by the operator through rhythmic probe pressure or may result from intrinsic physiological motion such as arterial pulsation. When stress is applied, softer tissues undergo greater deformation, whereas stiffer tissues exhibit reduced displacement [17]. The ultrasound system tracks pre- and post-compression echo signals to calculate relative displacement within the tissue. These relative strain differences are then displayed as qualitative or semi-quantitative color-coded maps, overlaying the grayscale image. Conventionally, red represents softer regions, blue represents stiffer regions, and intermediate colors denote varying elasticity levels, although color scales may differ across vendors [18]. Despite its clinical utility, strain elastography has inherent limitations. It does not directly measure tissue stiffness; rather, it estimates relative deformation within a field of view. Therefore, it provides comparative information rather than absolute values. The technique is highly operator-dependent, as the magnitude and uniformity of applied compression influence the resulting strain map. Excessive pressure may artificially increase stiffness readings, whereas insufficient compression reduces sensitivity. Additionally, strain measurements are affected by lesion depth, size, and surrounding tissue characteristics, limiting reproducibility across different examinations and operators [16–18]. These limitations prompted the development of more objective elastographic technologies.

3.2. Shear Wave Elastography

Shear wave elastography represents a significant technological advancement that addresses the reproducibility and quantification challenges of strain-based methods [19]. Rather than relying on manual compression, shear wave elastography utilizes focused acoustic radiation force impulses generated by the ultrasound transducer to

induce localized tissue displacement. This focused energy creates transient mechanical perturbations within the tissue, generating transverse shear waves that propagate perpendicular to the direction of the ultrasound beam. The velocity of these shear waves depends on tissue stiffness: stiffer tissues permit faster shear wave propagation, whereas softer tissues allow slower wave transmission [20–22]. By ultrafast imaging techniques, modern ultrasound systems track the speed of shear wave propagation in real time. The result is a quantitative, operator-independent stiffness map combined with numerical values obtained from user-defined regions of interest. This quantitative capability significantly enhances reproducibility and enables objective interpatient and longitudinal comparisons. Furthermore, shear wave elastography provides spatial visualization of stiffness heterogeneity within lesions, which may reflect tumor architecture, necrotic regions, or stromal distribution. Nevertheless, shear wave elastography is not entirely free from technical considerations. Measurements may be influenced by lesion depth, anisotropy of tissue fibers, presence of calcifications, cystic components, and patient motion [23]. Furthermore, variability between manufacturers in pulse generation and processing algorithms can lead to differences in absolute stiffness values (**Figure 1**).

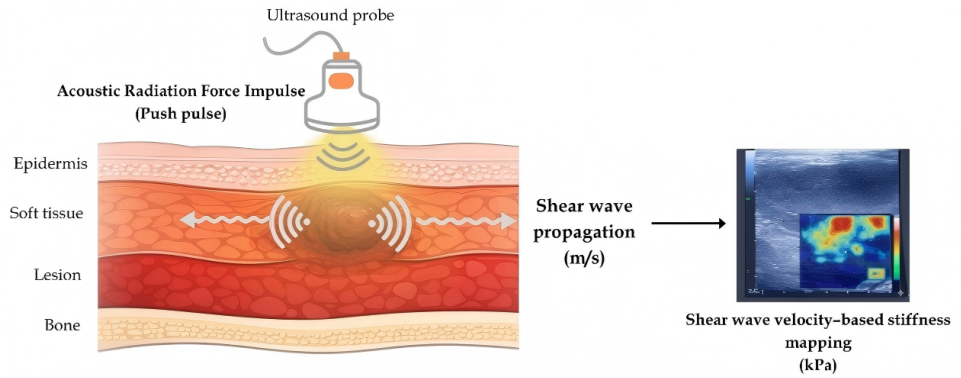

Figure 1. Mechanism of shear wave elastography.

4. Quantitative Metrics in Shear Wave Elastography

Shear wave elastography has advanced elastographic imaging from qualitative stiffness mapping (done in strain elastography) to a quantitative measurement platform. Its principal strength lies in the generation of reproducible numerical parameters that characterize tissue mechanical properties. These quantitative outputs allow objective comparison across examinations, facilitate longitudinal monitoring, and support statistical modeling frameworks required for biomarker validation.

4.1. Shear Wave Velocity

The fundamental parameter measured in shear wave elastography is shear wave velocity, expressed in meters per second (m/s). Acoustic radiation force impulses generated by the transducer induce localized tissue displacement, producing transverse shear waves that propagate through the medium. Ultrafast imaging sequences track the temporal progression of these wave fronts, enabling direct calculation of propagation speed [24, 25]. Shear wave velocity reflects intrinsic tissue stiffness: increased stiffness permits faster propagation, whereas softer tissues demonstrate reduced velocity. As velocity is directly measured from wave tracking rather than mathematically derived, it represents the primary physical output of the technique. For this reason, reporting velocity values may reduce dependence on modeling assumptions inherent in elasticity conversion formulas. Accurate velocity estimation requires adequate signal quality, appropriate acquisition depth, and minimization of motion artifacts. Variations in transducer frequency, acquisition frame rate, and post-processing algorithms may influence measured values. Therefore, standardized acquisition parameters are essential for reproducibility.

4.2. Elastic Modulus Estimation and Young's Modulus

Most clinical systems convert measured shear wave velocity into elasticity values expressed in kilopascals (kPa), approximating Young's modulus [24]. This conversion is based on the relationship between shear modulus

(μ), shear wave velocity (c), and tissue density (ρ):

$$\mu = \rho c^2$$

Young's modulus (E) can be approximated as:

$$E \approx 3\mu$$

These equations assume that tissue behaves as a homogeneous, isotropic, and linearly elastic medium. Under such assumptions, velocity measurements can be mathematically transformed into elasticity values that represent resistance to deformation. Biological tissues, however, exhibit viscoelastic and anisotropic properties. Their mechanical behavior may vary depending on directional fiber orientation and frequency of applied stress. Consequently, elasticity values derived from shear wave elastography should be interpreted as standardized stiffness indices rather than absolute biomechanical constants. Despite these theoretical constraints, kilopascal measurements provide clinically interpretable numerical values that facilitate threshold determination and comparative analysis.

4.3. Region of Interest–Based Statistical Parameters

Quantitative assessment in shear wave elastography relies on region of interest placement within the imaged field [26]. Systems generally allow circular or customizable ROI (Region of Interest) selection, from which statistical parameters are calculated. Commonly reported metrics include mean elasticity, median elasticity, maximum elasticity, minimum elasticity, and standard deviation within the selected ROI. Mean elasticity provides an overall estimate of tissue stiffness within the sampled area. Maximum elasticity may reflect focal regions of increased mechanical resistance, while standard deviation offers insight into stiffness variability within the tissue. Thus, proper ROI placement is critical for accurate quantification. Inclusion of areas affected by acoustic shadowing, reverberation artifacts, or structural heterogeneity can significantly alter these ROI-based measurements. Consistency in ROI size, depth, and placement improves reproducibility across examinations [27–29].

4.4. Relative Stiffness Indices and Ratio Measurements

To account for inter-individual variability in baseline tissue stiffness, relative stiffness indices may be calculated. These indices compare the elasticity of a target region to that of adjacent reference tissue within the same imaging plane. Ratio-based measurements can partially mitigate variability arising from patient-specific characteristics or machine calibration differences. However, the reliability of ratio measurements depends on the stability and homogeneity of the selected reference tissue. Variability in reference region properties may influence calculated ratios, underscoring the need for consistent methodological protocols [30].

4.5. Stiffness Distribution and Advanced Quantitative Analysis

Shear wave elastography generates spatial stiffness maps that allow evaluation of mechanical heterogeneity within tissue. Beyond single summary statistics, distribution-based metrics derived from elasticity maps are increasingly explored. These include percentile values, variance, skewness, and kurtosis of stiffness distributions. Such parameters characterize the internal mechanical architecture of tissue and may provide additional discriminatory information beyond mean stiffness values. Histogram-based analysis and texture quantification represent evolving approaches that facilitate integration of elastographic data into radiomics and computational modeling frameworks.

4.6. Technical Determinants of Measurement Variability

Although shear wave elastography provides objective numerical output, several technical and biological factors influence quantitative accuracy. These include lesion depth, tissue anisotropy, transducer frequency, probe precompression, patient motion, and signal attenuation. Differences in pulse generation strategies and reconstruction algorithms across manufacturers may also lead to variability in reported elasticity values. Standardization of acquisition protocols, including patient positioning, minimal transducer pressure, consistent ROI placement, and quality map assessment, is essential to enhance reproducibility. For shear wave elastography to function as a vali-

dated imaging biomarker, quantitative metrics must demonstrate reliability across observers, systems, and clinical environments [31].

5. Clinical Applications of Shear Wave Elastography in Head and Neck Imaging

Shear wave elastography has increasingly been integrated into routine ultrasonographic evaluation of head and neck structures. Its ability to provide quantitative stiffness measurements complements grayscale morphology and Doppler vascularity assessment, contributing an additional biomechanical dimension to lesion characterization. In anatomically complex regions where tissue heterogeneity is common and morphological overlap between benign and malignant entities is frequent, stiffness quantification has demonstrated incremental diagnostic value.

5.1. Thyroid Gland

The thyroid gland represents the most extensively studied application of shear wave elastography in head and neck imaging. Conventional ultrasound-based risk stratification systems rely on morphological features such as hypoechogenicity, irregular margins, microcalcifications, and taller-than-wide configuration. However, significant overlap persists between benign hyperplastic nodules, inflammatory lesions, and differentiated thyroid carcinomas, limiting specificity and leading to unnecessary biopsies in indeterminate cases [32,33]. Shear wave elastography introduces a quantitative biomechanical parameter that correlates with histopathological architecture. Increased stiffness in malignant nodules is primarily attributed to hypercellularity, desmoplastic stromal reaction, extracellular matrix remodeling, and increased interstitial pressure. This biological rationale is consistently supported by prospective clinical investigations. For instance, Tuan et al. demonstrated significantly higher elasticity indices in malignant nodules compared with benign lesions, reporting an area under the receiver operating curve (AUROC) of 0.889 using a 74.5 kPa threshold [34]. Similarly, Hazem et al., in a pediatric and adolescent cohort, reported excellent diagnostic performance with an area under the curve (AUC) of 0.921 and identified 42.2 kPa as an optimal cut-off value, with sensitivity exceeding 85% and specificity approaching 95%. Liao et al. confirmed that a mean SWE value ≥ 32 kPa functioned as an independent predictor of malignancy, with an odds ratio of 16.8 in multivariate analysis [35]. Despite consistent demonstration that malignant nodules are stiffer than benign nodules, reported cut-off values vary considerably across studies. Petersen et al. identified a lower optimal threshold of 18.5 kPa, achieving high negative predictive value but moderate specificity, and showed that combining SWE with Thyroid Imaging Reporting and Data System (TIRADS) significantly improved overall diagnostic accuracy compared with TIRADS alone [36]. In a larger prospective cohort, Mena et al. reported mean elasticity cut-offs around 47.5 kPa and maximum elasticity values exceeding 100 kPa when using 2D-SWE and point-SWE techniques, further illustrating methodological variability [37]. These discrepancies likely reflect differences in vendor-specific reconstruction algorithms, ROI selection strategies, lesion depth, use of mean versus maximum stiffness parameters, and background thyroid parenchymal status. Importantly, while stiffness thresholds differ numerically, diagnostic performance metrics remain consistently favorable, with most studies reporting good to excellent AUC values. The reproducible finding across heterogeneous populations is not a universal elasticity number, but rather a consistent directional increase in stiffness in malignant nodules.

Beyond focal nodules, shear wave elastography has also demonstrated utility in diffuse thyroid disease. Kara et al. reported significantly elevated parenchymal stiffness in patients with Hashimoto's thyroiditis compared with healthy controls and proposed a threshold of approximately 29 kPa for identifying autoimmune involvement. Stiffness values correlated positively with autoantibody titers and glandular volume, suggesting that SWE may serve as a quantitative surrogate of fibrosis and inflammatory remodeling. However, increased background stiffness in autoimmune thyroiditis may reduce specificity when evaluating coexisting nodules [38]. Collectively, current evidence indicates that shear wave elastography enhances thyroid nodule characterization, particularly when integrated with grayscale risk stratification systems. While absolute cut-off values remain institution- and vendor-dependent, stiffness quantification consistently improves specificity and may aid in the evaluation of indeterminate nodules. Standardization of acquisition protocols and multicenter validation remain necessary before universal threshold adoption can be recommended. In addition to cancer risk stratification, SWE can also be used in active surveillance programs for low-risk thyroid cancer and follow-up programs for diffuse thyroid disease. Quantitative stiffness assessment could complement existing ultrasound-based risk stratification systems and reduce unneces-

sary fine-needle aspiration procedures in selected patients. To facilitate comparison among published studies and highlight the variability in reported diagnostic thresholds and performance metrics, a summary of major SWE studies evaluating thyroid lesions is provided in **Table 1**.

Table 1. Comparative Summary of Shear Wave Elastography (SWE) Parameters for Thyroid Disorders.

Study (Author & Year)	Sample Size (n)	Population Cohort	Ultrasound System Hardware	SWE Technique	ROI Strategy	Cut-Off Value (kPa)	Sensitivity (%)	Specificity (%)	Area under Curve (AUC)
Tuan et al. (2020) [34]	86 patients (94 nodules)	Adults	LOGIQ S8 XDclear 2.0	2D-SWE (via ARFI)	Average of 5 sequential longitudinal measurements across the entire acquisition box	74.5 kPa	74.3%	90.0%	0.889
Hazem et al. (2021) [35]	56 patients (72 nodules)	Pediatric (Children & Adolescents, 11–19 yrs)	Philips EPIQ 7G	2D-SWE	2 × 2 mm ROI targeted strictly at the stiffest solid area (avoiding calcifications/cystic shifts); average of 3 scans	42.2 kPa (SWE-Mean)	85.71%	94.83%	0.921
Petersen et al. (2022) [36]	43 patients (61 nodules)	Adults (Pre-surgical)	GE Logiq S9	2D-SWE	Fixed ROI placed in the nodule vs. adjacent normal tissue to calculate the mean Young's modulus; 3 scans	18.5 kPa	80.0%	49.0%	Not explicitly isolated
Mena et al. (2023) [37]	170 nodules	Mixed/General	Mindray Resona 7	Dual-Evaluation: 1. 2D-SWE (Real-Time)	Small 3 × 3 mm or 5 × 5 mm ROI sample windows positioned at an optimal target depth of 1.2 to 1.5 cm	47.5 kPa (2D-SWE Mean)	81.2%	57.6%	Utilized in ROC models
				2. point-SWE (pSWE)		52.4 kPa (pSWE Average)	81.2%	57.6%	

5.2. Salivary Glands

Salivary gland pathology encompasses a broad spectrum of focal neoplasms and diffuse inflammatory or autoimmune disorders. Conventional ultrasound remains the primary imaging modality, providing information regarding lesion morphology, vascularity, and ductal changes [10,39]. However, structural imaging alone often cannot reliably distinguish between tumor subtypes or quantify the extent of parenchymal involvement in inflammatory disease. This limitation has prompted exploration of shear wave elastography as a quantitative adjunct capable of objectively assessing tissue stiffness. In focal salivary gland masses, stiffness differences reflect underlying histological composition. Pleomorphic adenomas, characterized by fibrous and myxochondroid stromal elements, tend to exhibit relatively increased stiffness compared with more cystic or lymphoid-rich lesions such as Warthin tumors [40]. Malignant salivary tumors often demonstrate further elevation in stiffness, attributable to increased cellular density and desmoplastic stromal response. Nevertheless, significant overlap exists among tumor subtypes, limiting the reliability of stiffness as a solitary discriminator. Current evidence suggests that shear wave elastography should therefore be interpreted as a complementary parameter that refines morphological assessment rather than replaces it [41]. The utility of shear wave elastography becomes more pronounced in diffuse inflammatory and autoimmune disorders of the salivary glands. Chronic inflammatory conditions are associated with progressive fibrosis and architectural distortion, leading to measurable increases in tissue stiffness. Elbeblawy and Mohamed demonstrated significantly higher shear wave velocity values in patients with chronic inflammatory salivary disease compared with healthy controls, identifying a cut-off around 23.5 kPa with moderate diagnostic accuracy [42]. In a prospective controlled study, Atik et al. reported significantly increased stiffness in both parotid and submandibular glands of patients with ankylosing spondylitis presenting with sicca symptoms compared with healthy individuals. Importantly, intra- and interobserver reliability values were high, highlighting the reproducibility of SWE in this context. Although histopathological correlation was not available in that study, the increased stiffness likely reflects subclinical inflammatory infiltration and early fibrotic remodeling [43]. Normative reference values are essential for interpreting pathological elevation. Tanabe et al. provided control data for parotid glands, reporting mean shear elastic modulus values around 7–8 kPa in individuals without salivary gland disease, with no significant association with age, gender, or internal architecture [44]. This finding is clinically important, as it suggests that substantial stiffness elevation above this baseline is more likely attributable to disease-related structural alteration rather than demographic variation. Shear wave elastography also demonstrates dynamic applicability in obstructive pathology. In patients with sialolithiasis, Chang and Wang showed that the affected glands exhibited significantly higher shear wave velocity compared with contralateral normal glands prior to intervention [45]. Following successful interventional sialendoscopy, stiffness values decreased significantly, although short-term follow-up revealed persistent but reduced elevation compared with the normal side. This pattern suggests that ductal obstruction induces reversible parenchymal stiffness changes, and that SWE can objectively monitor post-treatment recovery beyond purely symptomatic assessment. The major studies evaluating the diagnostic and monitoring applications of shear

wave elastography in salivary gland pathology are summarized in **Table 2**.

Table 2. Shear Wave Elastography in Salivary Gland Disorders.

Study & Clinical Domain	Sample Size (n) & Cohort	SWE/Elastography Technique	ROI Sizing & Placement Strategy	Key Diagnostic Thresholds/Baseline Values	Core Findings
Wang and Jiang (2021) Neoplastic Differentiation [41]	56 patients: 1. 10 malignant tumors 2. 27 pleomorphic adenomas (PA) 3. 11 adenolymphomas/Warthin tumors (AL) 4. 8 other benign tumors	2D-SWEStiffness reported as Young's modulus (kPa)	Multi-point evaluation targeting both lesion center and peripheral margins	1. Maximum Young's modulus cut-off: 32.4 kPa 2. AUC: 0.805 3. Sensitivity: 90.9% 4. Specificity: 74.1%	SWE demonstrated good diagnostic performance in differentiating pleomorphic adenomas from Warthin tumors. However, substantial overlap in stiffness values between benign and malignant tumors limited its utility as a stand-alone tool for malignancy discrimination.
Elbeblawy and Mohamed (2020) Chronic Obstructive & Autoimmune Inflammation [42]	42 subjects: 1. 21 chronic inflammatory cases (15 Sjögren's syndrome, 4 recurrent parotitis, 2 sialolithiasis) 2. 21 healthy controls	Point-SWE (pSWE) using ARFI pulses Parallel strain elastography (SE)	4 mm circular ROI.Target ROI placed within representative glandular parenchyma; reference ROI positioned in masseter muscle (parotid) or subcutaneous tissue (submandibular)	1. SWE cut-off: 23.5 kPa 2. AUC: 0.819 3. Sensitivity: 81.0% 4. Specificity: 76.2% 5. Strain ratio cut-off: 1.13 6. AUC: 0.954 7. Sensitivity: 95.2% 8. Specificity: 100%	Both SWE and strain elastography differentiated diseased glands from healthy controls. Strain ratio demonstrated superior diagnostic performance compared with quantitative SWE. Neither technique reliably differentiated specific inflammatory disease subtypes.
Atik et al. (2025) Subclinical Autoimmune Infiltration [43]	137 subjects: 1. 66 ankylosing spondylitis patients with sicca symptoms 2. 71 healthy controls	Quantitative 2D-SWEStiffness reported in kPa	Three 1 mm circular ROIs positioned within homogeneous central glandular parenchyma while avoiding vessels, lymph nodes, and gland margins	Left parotid: >25.63 kPa (AUC: 0.768) Right parotid: >25.41 kPa (AUC: 0.656) Left submandibular: >20.80 kPa (AUC: 0.719) Right submandibular: >20.12 kPa (AUC: 0.690)	SWE detected salivary gland involvement before morphological abnormalities became visible on conventional ultrasonography. The technique may help identify patients requiring further evaluation while reducing unnecessary salivary gland biopsies.
Tanabe et al. (2025) Healthy Baseline Reference Data [44]	124 parotid glands from 62 oral cancer patients evaluated before radiotherapy or chemotherapy	Quantitative 2D-SWEStiffness reported in kPa	Multiple manual ROI placements within unaffected parotid parenchyma	Mean reference stiffness: 7.69 ± 2.29 kPa Range: 3.7–14.5 kPa	Established normative reference values for healthy parotid gland tissue. Stiffness showed no significant association with age, sex, or internal glandular architecture.
Chang and Wang (2023) Longitudinal Surgical Monitoring [45]	17 patients (15 submandibular, 2 parotid glands) Total measurements: 1,709 (810 preoperative; 899 postoperative)	Point-SWE (pSWE) using ARFI trackingStiffness reported as shear wave velocity (m/s)	10–15 measurements per gland obtained from central parenchyma at a depth of 1.0–1.5 cm while avoiding stones, vessels, and bone	Significant postoperative reduction in shear wave velocity (p = 0.001; 95% CI: −0.39 to −0.20 m/s)	SWE effectively monitored recovery following sialendoscopy. Persistent stiffness elevation after symptom resolution suggested delayed parenchymal remodeling, while early increases in stiffness predicted secondary ductal stenosis.

5.3. Cervical Lymph Nodes

Evaluation of cervical lymphadenopathy remains a common and clinically significant challenge in head and neck imaging. Conventional ultrasound assessment relies on morphological criteria such as nodal shape, short-axis diameter, cortical thickness, loss of fatty hilum, and vascular pattern [11,46]. While these features improve diagnostic suspicion, overlap between reactive, inflammatory, metastatic, and lymphoproliferative conditions frequently limits specificity. In this context, shear wave elastography offers an additional biomechanical parameter that reflects structural alterations within nodal architecture. The stiffness of a lymph node is largely determined by its internal composition. Reactive lymph nodes preserve their normal architecture, including a central fatty hilum and organized cortical tissue. In contrast, metastatic involvement often results in cortical infiltration, desmoplastic stromal reaction, and increased cellular density, leading to measurable stiffening. Several clinical investigations have demonstrated that metastatic lymph nodes exhibit significantly higher elasticity values than benign reactive nodes [47,48]. Reported stiffness values in malignant nodes frequently exceed those of benign nodes, and receiver operating characteristic analyses in multiple cohorts have shown good to excellent discriminatory performance. Areas of central necrosis within metastatic nodes may reduce the measured stiffness if the region of interest includes liquefactive components. Conversely, chronic inflammatory nodes with fibrosis may exhibit increased stiffness, potentially mimicking malignant infiltration. Therefore, accurate region-of-interest placement, avoiding necrotic zones and calcifications, is essential for reliable interpretation [49,50]. Shear wave elastography has also been investigated in lymphoproliferative disorders. In lymphoma, nodal stiffness patterns may differ from metastatic carcinoma due to the absence of desmoplastic reaction and the presence of diffuse cellular proliferation [51]. Some studies suggest intermediate stiffness values in lymphoma compared with metastatic nodes, although overlap persists. These findings indicate that while elastography contributes valuable information, it cannot independently determine histologic subtype. Beyond diagnostic differentiation, shear wave elastography may have a role in treatment monitoring. Post-radiotherapy or post-chemotherapy nodes often undergo fibrotic remodeling, leading to increased stiffness independent of viable tumor presence. Serial stiffness assessment, when interpreted alongside morphological evolution, may provide additional insight into therapeutic response [52]. However, longitudinal thresholds remain under investigation (**Table 3**).

Table 3. Summary of Major Studies Evaluating Shear Wave Elastography in Cervical Lymph Nodes.

Study & Clinical Domain	Sample Size (n) & Cohort	Ultrasound System & Hardware	SWE/Elastography Technique	ROI Sizing & Placement Strategy	Key Diagnostic Thresholds/Baseline Values	Core Findings
Termure et al. (2025) Malignant Stratification (Lymphoma vs. Metastasis) [47]	80 lymph nodes from 70 patients: 1. 39 benign nodes 2. 14 primary lymphomas 3. 27 metastatic nodes	Standardized electronic linear array tracking system	Quantitative 2D-SWEYoung's modulus reported in kPa	ROIs placed within central nodal parenchyma using real-time color elasticity maps while avoiding peripheral compression zones and adjacent vascular structures	Mean Stiffness Values: 1. Benign: 17.7 ± 5.42 kPa 2. Lymphoma: 70.6 ± 27.96 kPa 3. Metastasis: 122.8 ± 77.40 kPa	Established a clear stiffness hierarchy between benign, lymphomatous, and metastatic nodes. Progressive stiffness elevation was strongly associated with metastatic disease and reflected increasing stromal desmoplastic remodeling.
Azizi et al. (2016) Predicting Nodal Malignancy via Velocity Staging [48]	270 lymph nodes from 231 patients: 1. 216 benign nodes 2. 54 malignant nodes	Siemens ACUSON S30009L4 Multi-D linear array transducer	Quantitative SWE using Virtual Touch Imaging Quantification (VTIQ) Shear wave velocity (m/s)	Fixed 1.5 mm software ROI positioned over the stiffest nodal region identified on velocity maps and sampled twice to obtain maximum SWV	Mean SWV: 1. Benign: 2.71 ± 0.65 m/s 2. Malignant: 3.96 ± 0.96 m/s Optimal Cut-off: 2.93 m/s AUC: 0.88 Sensitivity: 92.6% Specificity: 75.5% NPV: 97.6%	Demonstrated that VTIQ-derived velocity is a powerful predictor of nodal malignancy. A threshold of 2.93 m/s provided excellent negative predictive value, supporting its use as a non-invasive rule-out tool.
Sun et al. (2022) Multi-Parametric Mechanical Profiling [49]	204 patients: 1. 80 benign nodes 2. 26 lymphoma nodes 3. 98 metastatic nodes	Multi-frequency superficial linear transducer system	Quantitative SWEElastic modulus (kPa) and shear wave velocity (m/s)	ROIs positioned within representative central nodal parenchyma while avoiding artifacts and adjacent muscular or osseous structures	Elastic Modulus Cut-off: 42.90 kPa AUC: 0.976 Sensitivity: 92.7% Specificity: 97.5% Velocity Cut-off: 3.73 m/s AUC: 0.970 Sensitivity: 92.7% Specificity: 96.3%	Demonstrated a progressive increase in stiffness from benign nodes to lymphoma and metastatic disease. Combining SWE metrics with conventional ultrasonography significantly improved diagnostic performance.
Wang et al. (2021) Technical Review and Structural Mapping [50]	Comprehensive review of published elastography literature	Multiple SE, pSWE, and 2D-SWE platforms	Comparative evaluation of strain elastography, point-SWE, and 2D-SWE	Emphasized optimized ROI placement within cortical and medullary nodal regions and standardization of acquisition protocols	Reviewed strain ratios, Young's modulus values (kPa), and shear wave velocity measurements (m/s)	Highlighted the biomechanical basis of nodal stiffness variation and identified quantitative SWE as the most objective and reproducible elastographic technique for lymph node assessment.
Chae et al. (2019) Differentiation of Lymphoma and Metastatic Nodes [51]	Patients with confirmed malignant cervical lymphadenopathy	High-resolution ultrasound with acoustic radiation force tracking software	Quantitative 2D-SWE Young's modulus reported in kPa	Real-time color-coded elasticity maps combined with quantitative stiffness measurements to evaluate nodal heterogeneity	Quantitative and qualitative elasticity patterns used to distinguish metastatic carcinoma from lymphoma	Demonstrated distinct elastographic signatures between lymphoma and metastatic disease. Metastatic nodes exhibited higher stiffness and greater heterogeneity, whereas lymphomatous nodes showed comparatively lower stiffness due to the absence of marked desmoplastic stromal reaction.

5.4. Oral Structures

Shear wave elastography has expanded the scope of ultrasonographic evaluation in the oral and maxillofacial region beyond static lesion characterization to include functional muscle assessment and periodontal tissue monitoring. The oral cavity presents technical challenges due to limited acoustic windows and motion artifacts. However, high-frequency linear probes allow reliable evaluation of superficial soft tissues. In this setting, shear wave elastography provides quantitative stiffness measurements that reflect structural and functional tissue properties. In focal oral lesions, stiffness values correlate with underlying histopathological architecture. Ogura et al. demonstrated that squamous cell carcinomas exhibited markedly elevated shear elastic modulus values compared with benign oral lesions. Malignant lesions showed substantially higher stiffness, while healthy sublingual gland and floor-of-mouth structures demonstrated low baseline elasticity. These findings support the biological premise that malignant transformation, characterized by cellular proliferation and desmoplastic stromal reaction, results in measurable mechanical stiffening. Although limited by small sample size, this study established the feasibility of SWE as a quantitative adjunct for differentiating malignant from benign oral soft tissue lesions [53]. Beyond tumor characterization, shear wave elastography provides a unique window into masticatory muscle biomechanics. Olchowy et al. demonstrated that stiffness of the masseter and temporalis muscles increased significantly following short-term intensive chewing and partially returned toward baseline after relaxation. The masseter muscle consistently exhibited higher stiffness than the temporalis muscle, and stiffness values between muscles were positively correlated [54]. These findings confirm that SWE is sensitive to dynamic physiological changes in muscle tone and contraction. Clinically, this has implications for evaluating parafunctional habits, bruxism, and temporomandibular disorders, where objective quantification of muscle overactivity has historically been limited. Elastography may therefore serve as a functional biomarker of masticatory muscle workload and recovery. An additional and novel application is in periodontal tissue assessment. Gingival firmness has traditionally been evaluated subjectively during clinical examination, without quantitative measurement. Xue et al. investigated the use of shear wave elastography to monitor gingival elasticity in patients with advanced periodontitis undergoing initial periodontal therapy [55]. Baseline gingival stiffness values were lower in inflamed tissues and demonstrated negative correlation with plaque index and gingival bleeding index, indicating that active inflammation was associated with

reduced mechanical integrity. Following periodontal therapy, stiffness values increased significantly, reflecting tissue healing and improved gingival firmness. These changes were most pronounced during the early postoperative period and correlated with baseline stiffness measurements. This study highlights the potential of SWE as a real-time, non-invasive biomarker of periodontal tissue remodeling and therapeutic response. Despite these promising findings, the application of shear wave elastography in oral tissues for diagnosis of oral diseases remains in an early stage of development. Current evidence is limited by small sample sizes, heterogeneous imaging protocols, and a lack of standardized stiffness reference values for oral soft tissues. Furthermore, anatomical constraints within the oral cavity, including limited probe access, variable tissue thickness, and susceptibility to motion artifacts, continue to pose technical challenges. Future studies involving larger cohorts and standardized acquisition protocols are required to establish normative stiffness values and validate the diagnostic and prognostic utility of SWE in oral lesions, masticatory muscle disorders, and periodontal diseases.

5.5. Temporomandibular Joint (TMJ)

The application of shear wave elastography to temporomandibular joint disorders represents one of the most technically innovative extensions of ultrasound elastography in head and neck imaging. Conventional evaluation of the TMJ relies on MRI for disc morphology and position, and CBCT for osseous changes [56]. However, neither modality provides quantitative assessment of tissue biomechanics. Shear wave elastography introduces the possibility of measuring mechanical properties of both the articular disc and masticatory musculature in real time. The temporomandibular disc is a fibrocartilaginous structure whose mechanical integrity is central to joint function. Alterations in disc position and degeneration are hallmarks of temporomandibular disorders (TMDs). Paluch et al. demonstrated that patients with TMDs exhibit region-specific alterations in disc stiffness. In their study, the intermediate zone of the disc showed significantly increased stiffness, whereas the anteriorly displaced portion demonstrated significantly reduced stiffness compared with healthy controls. Notably, a decrease in stiffness of the anteriorly displaced disc portion below 8.667 kPa provided extremely high diagnostic accuracy, with near-perfect sensitivity and specificity in distinguishing TMD patients from controls. Conversely, increased stiffness of the intermediate zone above 54.33 kPa demonstrated high specificity but limited sensitivity. These findings suggest that disc displacement is associated not only with positional change but also with measurable biomechanical remodeling. Normative data are essential for contextual interpretation [57]. Öztürk et al. evaluated disc stiffness in healthy children and adolescents and demonstrated that the posterior disc region is physiologically less stiff than anterior and intermediate portions. Importantly, disc stiffness values were higher in the open mouth position compared with the closed mouth position, reflecting physiological loading. No significant association with age, height, weight, or BMI was observed. These baseline data establish physiological variation across disc regions and jaw positions, allowing differentiation between normal biomechanical variability and pathological alteration [58]. Collectively, these studies suggest that shear wave elastography can detect region-specific disc remodeling associated with displacement and degeneration. However, reproducibility across different ultrasound systems and standardized probe positioning remain challenges. Beyond the intra-articular disc, masticatory muscle dysfunction is a major contributor to temporomandibular disorders. Shear wave elastography offers quantitative assessment of muscle stiffness under dynamic conditions. Functional studies in healthy adults have shown that masseter and temporalis muscle stiffness increases significantly following chewing activity and decreases after relaxation, confirming that SWE is sensitive to physiological muscle contraction [54,59,60]. In bruxism, altered stiffness patterns have been observed. Proof-of-principle investigations demonstrated that masseter stiffness at rest is significantly elevated in bruxism patients compared with controls. During maximal mouth opening, however, bruxism patients exhibited lower stiffness values than controls, likely reflecting limited jaw excursion and altered muscular biomechanics. Some studies have proposed stiffness thresholds for identifying bruxism-related muscle rigidity, though variability between protocols remains substantial. They concluded that while shear wave elastography in bruxism is feasible and promising, methodological standardization and larger validation cohorts are required before routine clinical adoption [61,62]. Factors such as region-of-interest size, jaw position, bite force standardization, and time averaging significantly influence measurements. Normative reference values for masseter stiffness in healthy adults and children have been reported, demonstrating higher stiffness during open mouth or active contraction compared with relaxed conditions. These physiological variations emphasize the importance of standardized acquisition conditions when interpreting pathological elevation. However, several limitations remain when using SWE for TMJ.

The TMJ disc is small and deep, requiring precise probe positioning. Anisotropic properties of fibrocartilage and muscle fibers may affect measurements. Dynamic jaw positioning significantly alters stiffness values, necessitating strict protocol standardization. Moreover, while some studies report remarkably high diagnostic accuracy, external validation and multicenter replication are limited. The ability of SWE to quantify both intra-articular and muscular biomechanical alterations offers a unique advantage over conventional imaging modalities. Future incorporation of SWE into multimodal TMJ assessment protocols may improve diagnosis, disease staging, and monitoring of therapeutic outcomes in patients with temporomandibular disorders (**Table 4**).

Table 4. Shear Wave Elastography in Temporomandibular Joint and Masticatory Muscle Disorders.

Study	Population	Anatomical Target	SWE Protocol/ROI Placement	Principal SWE Findings	Clinical Relevance
Paluch et al., (2020) [57]	37 TMD patients and 208 healthy controls	TMJ disc	Three ROIs placed within the intermediate zone (ROI1), transitional zone (ROI2), and anteriorly displaced disc portion (ROI3)	TMD patients exhibited significantly increased stiffness in the intermediate disc region (36.7 ± 4.6 kPa) and markedly reduced stiffness in the anteriorly displaced portion (4.5 ± 2.1 kPa). ROI3 stiffness < 8.667 kPa showed excellent diagnostic accuracy (AUC 0.999).	Demonstrated the feasibility of SWE as a non-invasive diagnostic tool for TMJ disc displacement and internal derangement.
Öztürk et al., (2021) [58]	123 healthy children and adolescents	TMJ disc and masseter muscle	Three ROIs placed in anterior, middle, and posterior disc regions; masseter assessed in open- and closed-mouth positions	Posterior disc stiffness was significantly lower than anterior and middle regions. Masseter stiffness increased significantly during mouth opening (16.96 ± 9.01 kPa closed mouth vs. 28.7 ± 10.2 kPa open mouth).	Established normative pediatric SWE values for TMJ disc and masseter muscle assessment.
Olchowy et al., (2022) [59]	Patients undergoing conservative treatment for masticatory muscle disorders	Masseter muscle	SWE measurements performed longitudinally during treatment	Significant reduction in masseter stiffness following conservative therapy, paralleling clinical improvement.	Supports SWE as an objective tool for monitoring therapeutic response in masticatory muscle disorders.
Chen et al., (2023) [60]	Orofacial pain patients and healthy controls	Superficial and deep masseter; superficial and deep temporalis muscles	SWE and ultrasonographic thickness measurements obtained from four masticatory muscle compartments	Patients with orofacial pain demonstrated significantly increased muscle stiffness compared with controls. Stiffness changes were more discriminatory than muscle thickness measurements.	Suggests SWE may serve as a sensitive biomarker of masticatory muscle dysfunction associated with orofacial pain.
Güven et al., (2025) [61]	Bruxism patients and healthy controls	Masseter muscle	SWE evaluation of masseter muscle elasticity	Bruxism patients demonstrated significantly altered masseter stiffness compared with controls, reflecting chronic muscular overload.	Supports the use of SWE as an objective adjunctive diagnostic method for bruxism.

6. Limitations and Standardization Challenges in Shear Wave Elastography for Head and Neck

Despite its promising role as a quantitative imaging biomarker, shear wave elastography in head and neck imaging remains subject to several technical and methodological limitations. Measurement variability may arise from depth dependency, tissue anisotropy, probe precompression, motion artifacts, and heterogeneity within lesions. Inter-vendor differences in pulse generation, reconstruction algorithms, and elasticity conversion formulas contribute to substantial variability in reported stiffness thresholds across studies. Small anatomical structures such as the temporomandibular disc and superficial oral tissues require meticulous probe positioning and standardized acquisition protocols to ensure reproducibility. Furthermore, biological tissues are viscoelastic and anisotropic, meaning that reported kilopascal values represent modeled stiffness indices rather than absolute biomechanical constants. The absence of universally accepted acquisition parameters, calibration standards, and disease-specific cut-off values currently limits broader clinical standardization [63]. Addressing these challenges through consensus protocols, multicenter validation studies, and harmonized reporting guidelines will be essential for the integration of shear wave elastography into routine head and neck practice (**Table 5**).

Table 5. Technical Limitations and Standardization Challenges in Head and Neck Shear Wave Elastography.

Domain	Specific Limitation	Underlying Mechanism	Impact on Measurement	Clinical Consequence	Standardization/Research Need
Acoustic Physics	Depth dependency	Shear wave amplitude attenuates with depth	Underestimation in deep lesions	False reassurance in deep nodes or parotid lesions	Define validated depth ranges per anatomic site
	Frequency dependence	Different probe frequencies alter wave propagation	Inconsistent stiffness values	Cut-off variability between devices	Report probe frequency in all studies
	Limited penetration in calcified tissues	Acoustic shadowing blocks wave tracking	Falsely elevated or unreliable readings	Misclassification of calcified nodules	Exclusion of shadowed regions in ROI
	Cystic or necrotic components	Fluid transmits low shear resistance	Artificially low stiffness values	False-negative malignancy assessment	ROI restricted to solid components
Tissue Biomechanics	Anisotropy	Fiber orientation affects shear velocity	Direction-dependent variability	Inconsistent muscle and TMJ disc readings	Standardize probe alignment parallel to fibers
	Viscoelastic behavior	Time- and frequency-dependent stiffness	Model-based approximation errors	Non-universal kPa interpretation	Encourage reporting of both kPa and m/s
	Heterogeneous lesions	Mixed fibrosis, necrosis, inflammation	High intra-lesional variability	Reduced specificity	Incorporate heterogeneity indices

Table 5. *Cont.*

Domain	Specific Limitation	Underlying Mechanism	Impact on Measurement	Clinical Consequence	Standardization/Research Need
Operator Factors	Probe precompression	Excess manual pressure increases stiffness	Overestimation of elasticity	False-positive malignancy risk	Minimal pressure protocol guidelines
	ROI placement variability	Size, depth, and region differences	Measurement dispersion	Poor reproducibility	Standard ROI size per organ
	Jaw/muscle position inconsistency	Open vs. closed mouth alters stiffness	Dynamic variability	Misinterpretation in TMJ and muscle studies	Fixed acquisition position definitions
	Learning curve	Inexperience in wave quality assessment	Low interobserver agreement	Reduced reliability	Structured training programs
Patient-Related Factors	Motion artifacts	Swallowing, speaking, chewing	Unstable wave tracking	Invalid measurements	Standardized patient instructions
	Inflammation vs. fibrosis overlap	Both may elevate stiffness	Reduced diagnostic specificity	Misclassification of reactive tissue	Combine SWE with grayscale criteria
	Background parenchymal disease	Thyroiditis, sialadenitis elevate baseline stiffness	Altered lesion-to-background contrast	Reduced threshold reliability	Separate disease-specific reference ranges
Device and Algorithm Variability	Vendor-specific reconstruction algorithms	Proprietary signal processing	Wide cutoff variability (18–75+ kPa)	Poor inter-study comparability	Cross-vendor calibration studies
	Different ROI shapes and smoothing settings	Algorithm-dependent elasticity mapping	Altered stiffness distribution	Inconsistent reported thresholds	Standardized reporting of acquisition settings
	kPa conversion assumptions	Young's modulus derived from $\mu = \rho c^2$	Model-dependent stiffness estimation	Overinterpretation of absolute values	Encourage velocity-based reporting
Study Design Limitations	Small sample sizes	Limited statistical power	Overestimated diagnostic performance	Inflated sensitivity/specificity	Large multicenter trials
	Lack of histopathological correlation	Imaging not always biopsy-confirmed	Verification bias	Uncertain diagnostic validity	Mandatory histologic reference standard
	Cross-sectional designs	No longitudinal follow-up	Limited understanding of progression	Unclear therapeutic monitoring value	Prospective longitudinal studies
	Population heterogeneity	Age, sex, comorbidities	Baseline stiffness variation	Poor generalizability	Stratified normative databases
Clinical Implementation	Absence of universal cutoffs	Protocol and device heterogeneity	No global threshold	Limited guideline adoption	International consensus panels
	Lack of integration with multiparametric models	Isolated SWE interpretation	Reduced predictive accuracy	Overreliance on single metric	Standard multiparametric algorithms
	Reimbursement and workflow barriers	Limited clinical guidelines	Restricted adoption	Underutilization	Health economics validation studies

7. Conclusions

Shear wave elastography represents a significant advancement in quantitative ultrasound imaging of head and neck structures. By providing objective biomechanical measurements, it complements morphological assessment and enhances diagnostic specificity across multiple anatomical subsites. Harmonized acquisition protocols, cross-vendor calibration, and establishment of disease-specific normative databases are essential to enable reproducible multicenter application of shear wave elastography. Emerging advances such as three-dimensional elastography, higher-frequency probes for superficial structures, and real-time stiffness heterogeneity mapping may further enhance diagnostic precision. In addition, integration of elastographic parameters into multiparametric ultrasound models and radiomics frameworks offers opportunities for objective risk stratification and longitudinal disease monitoring. With continued validation and incorporation into structured clinical algorithms, shear wave elastography has the potential to evolve from an adjunctive tool into a validated quantitative biomarker in head and neck diagnostics.

Author Contributions

Conceptualization, S.S. and A.J.; methodology, S.S. and V.M.; validation, S.S., A.J., and V.S.; formal analysis, S.S.; resources, V.S. and V.M.; data curation, S.S., A.J., and V.S.; writing—original draft preparation, S.S., A.J., V.S., and V.M.; writing—review and editing, S.S., A.J., and V.S.; supervision, A.J. and V.M. All authors have read and agreed to the published version of the manuscript.

Funding

This work received no external funding.

Institutional Review Board Statement

Not applicable.

Informed Consent Statement

Not applicable.

Data Availability Statement

All data supporting the findings of this study are available within the paper.

Conflicts of Interest

The authors declare no conflict of interest.

AI Use Statement

During the preparation of this manuscript, the authors used Quillbot paraphraser solely for language refinement. No AI tools were used for data analysis, interpretation, or generation of scientific content. All outputs were critically reviewed and edited by the authors. The authors take full responsibility for the integrity and accuracy of the work.

References

1. Marcu, L.G.; Reid, P.; Bezak, E. The promise of novel biomarkers for head and neck cancer from an imaging perspective. *Int. J. Mol. Sci.* **2018**, *19*, 2511. [CrossRef]
2. Sham, M.E.; Nishat, S. Imaging modalities in head-and-neck cancer patients. *Indian J. Dent. Res.* **2012**, *23*, 819–821. [CrossRef]
3. Jha, A.K.; Mithun, S.; Sherkhane, U.B.; et al. Emerging role of quantitative imaging (radiomics) and artificial intelligence in precision oncology. *Explor. Target Antitumor Ther.* **2023**, *4*, 569–582. [CrossRef]
4. Taljanovic, M.S.; Gimber, L.H.; Becker, G.W.; et al. Shear-wave elastography: Basic physics and musculoskeletal applications. *Radiographics* **2017**, *37*, 855–870. [CrossRef]
5. Ooi, C.C.; Malliaras, P.; Schneider, M.E.; et al. "Soft, hard, or just right?" Applications and limitations of axial-strain sonoelastography and shear-wave elastography in the assessment of tendon injuries. *Skeletal Radiol.* **2014**, *43*, 1–12. [CrossRef]
6. Tang, A.; Cloutier, G.; Szeverenyi, N.M.; et al. Ultrasound elastography and MR elastography for assessing liver fibrosis: Part 1, principles and techniques. *AJR Am. J. Roentgenol.* **2015**, *205*, 22–32. [CrossRef]
7. Sarvazyan, A.; Hall, T.J.; Urban, M.W.; et al. An overview of elastography—An emerging branch of medical imaging. *Curr. Med. Imaging Rev.* **2011**, *7*, 255–282. [CrossRef]
8. Sultan, S.R. B-mode ultrasound characteristics of thyroid nodules with high-benign probability and nodules with risk of malignancy. *Cureus* **2023**, *15*, e39281. [CrossRef]
9. Țermure, D.A.; Badea, M.E.; Donci, D.D.; et al. Multimodal imaging of cervical lymphadenopathy: Diagnostic value and clinical applications. *Med. Pharm. Rep.* **2025**, *98*, 425–439. [CrossRef]
10. Koch, M.; Sievert, M.; Iro, H.; et al. Ultrasound in inflammatory and obstructive salivary gland diseases: Own experiences and a review of the literature. *J. Clin. Med.* **2021**, *10*, 3547. [CrossRef]
11. Raja Lakshmi, C.; Sudhakara Rao, M.; Ravikiran, A.; et al. Evaluation of reliability of ultrasonographic parameters in differentiating benign and metastatic cervical group of lymph nodes. *ISRN Otolaryngol.* **2014**, *2014*, 238740. [CrossRef]
12. Plaza-Manzano, G.; Fernández-de-Las-Peñas, C.; Díaz-Arribas, M.J.; et al. Diagnostic accuracy of ultrasound imaging and shear wave elastography to discriminate patients with chronic neck pain from asymptomatic individuals. *Healthcare* **2024**, *12*, 1987. [CrossRef]
13. Crespo, A.N.; Chone, C.T.; Fonseca, A.S.; et al. Clinical versus computed tomography evaluation in the diagnosis and management of deep neck infection. *Sao Paulo Med. J.* **2004**, *122*, 259–263. [CrossRef]
14. Charles-Edwards, E.M.; deSouza, N.M. Diffusion-weighted magnetic resonance imaging and its application to cancer. *Cancer Imaging* **2006**, *6*, 135–143. [CrossRef]
15. Ozturk, A.; Grajo, J.R.; Dhyani, M.; et al. Principles of ultrasound elastography. *Abdom. Radiol.* **2018**, *43*, 773–785. [CrossRef]
16. Kim, S.J.; Park, H.J.; Lee, S.Y. Usefulness of strain elastography of the musculoskeletal system. *Ultrasonography* **2016**, *35*, 104–109. [CrossRef]
17. Dietrich, C.F.; Dong, Y.; Cui, X.W.; et al. Ultrasound elastography: A brief clinical history of an evolving technique. *Ultrasound Int. Open* **2024**, *10*, a23786926. [CrossRef]
18. Dietrich, C.F.; Barr, R.G.; Farrokh, A.; et al. Strain elastography—How to do it? *Ultrasound Int. Open* **2017**, *3*, E137–E149. [CrossRef]
19. Alrashed, A.I.; Alfuraih, A.M. Reproducibility of shear wave elastography among operators, machines, and probes in an elasticity phantom. *Ultrasonography* **2021**, *40*, 158–166. [CrossRef]
20. Ličen, U.; Kozinc, Ž. Using shear-wave elastography to assess exercise-induced muscle damage: A review. *Sensors* **2022**, *22*, 7574. [CrossRef]

21. Lehoux, M.C.; Sobczak, S.; Cloutier, F.; et al. Shear wave elastography potential to characterize spastic muscles in stroke survivors: Literature review. *Clin. Biomech.* **2020**, *72*, 84–93. [CrossRef]
22. Ferraioli, G.; Barr, R.G.; Farrokh, A.; et al. How to perform shear wave elastography. Part I. *Med. Ultrason.* **2022**, *24*, 95–106. [CrossRef]
23. Bruce, M.; Kolokythas, O.; Ferraioli, G.; et al. Limitations and artifacts in shear-wave elastography of the liver. *Biomed. Eng. Lett.* **2017**, *7*, 81–89. [CrossRef]
24. Ryu, J.; Jeong, W.K. Current status of musculoskeletal application of shear wave elastography. *Ultrasonography* **2017**, *36*, 185–197. [CrossRef]
25. Cui, X.W.; Li, K.N.; Yi, A.J.; et al. Ultrasound elastography. *Endosc. Ultrasound* **2022**, *11*, 252–274. [CrossRef]
26. Xie, J.; Liu, H.; Liu, W.S.; et al. Quantitative shear wave elastography for noninvasive assessment of solid pancreatic masses. *Clin. Hemorheol. Microcirc.* **2020**, *74*, 179–187.
27. Cheng, K.L.; Lai, P.H.; Su, C.L.; et al. Impact of region-of-interest size on the diagnostic performance of shear wave elastography in differentiating thyroid nodules. *Cancers* **2023**, *15*, 5214. [CrossRef]
28. Ye, R.; Xiong, H.H.; Liu, X.; et al. The impact of different regions of interest on shear wave elastography assessment of the meniscus in the knee joint. *Acad. Radiol.* **2024**, *31*, 3306–3314. [CrossRef]
29. Moon, J.H.; Hwang, J.Y.; Park, J.S.; et al. Impact of region of interest size on the diagnostic performance of shear wave elastography in differentiating solid breast lesions. *Acta Radiol.* **2018**, *59*, 657–663. [CrossRef]
30. Kozinc, Ž.; Šarabon, N. Shear-wave elastography for assessment of trapezius muscle stiffness: Reliability and association with low-level muscle activity. *PLoS One* **2020**, *15*, e0234359. [CrossRef]
31. Ewertsen, C.; Carlsen, J.; Perveez, M.A.; et al. Reference values for shear wave elastography of neck and shoulder muscles in healthy individuals. *Ultrasound Int. Open* **2018**, *4*, E23–E29. [CrossRef]
32. Liu, Y.; Xu, W. Application and limitations of ultrasound for the early diagnosis of thyroid cancer: A systematic review and meta-analysis. *Am. J. Transl. Res.* **2025**, *17*, 6556–6572. [CrossRef]
33. Elaggan, A.; Mostafa, A.; Albdair, R.; et al. The value of ultrasonography using thyroid imaging reporting and data systems (TIRADS) in the diagnosis of thyroid cancer among the population of Ha'il, Saudi Arabia. *Cureus* **2022**, *14*, e27437. [CrossRef]
34. Tuan, P.A.; Duc, N.M.; An, M.; et al. The role of shear wave elastography in the discrimination between malignant and benign thyroid nodules. *Acta Inform. Med.* **2020**, *28*, 248–253. [CrossRef]
35. Hazem, M.; Zakaria, O.M.; Daoud, M.Y.I.; et al. Accuracy of shear wave elastography in characterization of thyroid nodules in children and adolescents. *Insights Imaging* **2021**, *12*, 128. [CrossRef]
36. Petersen, M.; Schenke, S.A.; Firla, J.; et al. Shear wave elastography and thyroid imaging reporting and data system (TIRADS) for the risk stratification of thyroid nodules—Results of a Prospective Study. *Diagnostics* **2022**, *12*, 109. [CrossRef]
37. Mena, G.; Montalvo, A.; Ubidia, M.; et al. Elastography of the thyroid nodule: Cut-off points between benign and malignant lesions for strain, 2D shear wave real time and point shear wave: A correlation with pathology, ACR TIRADS and Alpha Score. *Front. Endocrinol.* **2023**, *14*, 1182557. [CrossRef]
38. Kara, T.; Ateş, F.; Durmaz, M.S.; et al. Assessment of thyroid gland elasticity with shear-wave elastography in Hashimoto's thyroiditis patients. *J. Ultrasound* **2020**, *23*, 543–551. [CrossRef]
39. Astorri, E.; Sutcliffe, N.; Richards, P.S.; et al. Ultrasound of the salivary glands is a strong predictor of labial gland biopsy histopathology in patients with sicca symptoms. *J. Oral Pathol. Med.* **2016**, *45*, 450–454. [CrossRef]
40. Rong, X.; Zhu, Q.; Ji, H.; et al. Differentiation of pleomorphic adenoma and Warthin's tumor of the parotid gland: Ultrasonographic features. *Acta Radiol.* **2014**, *55*, 1203–1209. [CrossRef]
41. Wang, J.; Jiang, L. Application value of shear wave elastography in salivary gland tumors. *Oral Radiol.* **2021**, *37*, 653–657. [CrossRef]
42. Elbeblawy, Y.M.; Mohamed, M.E.A. Strain and shear wave ultrasound elastography in evaluation of chronic inflammatory disorders of major salivary glands. *Dentomaxillofac. Radiol.* **2020**, *49*, 20190225. [CrossRef]
43. Atik, I.; Atik, S.; Gul, E. Effectiveness of shear wave elastography for assessing major salivary gland involvement in ankylosing spondylitis. *Radiol. Bras.* **2025**, *58*, e20240121. [CrossRef]
44. Tanabe, Y.; Shirai, A.; Ogura, I. Shear wave elastography for parotid glands: Quantitative analysis of shear elastic modulus in relation to age, gender, and internal architecture in patients with oral cancer. *J. Imaging* **2025**, *11*, 145. [CrossRef]
45. Chang, C.F.; Wang, H.K. Ultrasound shear wave elastography for patients with sialolithiasis undergoing interventional sialendoscopy. *Laryngoscope Investig. Otolaryngol.* **2023**, *8*, 76–81. [CrossRef]
46. Ahuja, A.T.; Ying, M.; Ho, S.Y.; et al. Ultrasound of malignant cervical lymph nodes. *Cancer Imaging* **2008**, *8*,

48–56. [CrossRef]
47. Termure, D.A.; Lenghel, M.; Badea, M.E.; et al. Shear wave elastography for distinguishing cervical lymph node malignancy: A prospective, observational study. *Biomedicines* **2025**, *13*, 2001. [CrossRef]
48. Azizi, G.; Keller, J.M.; Mayo, M.L.; et al. Shear wave elastography and cervical lymph nodes: Predicting malignancy. *Ultrasound Med. Biol.* **2016**, *42*, 1273–1281. [CrossRef]
49. Sun, Y.; Wang, W.; Mi, C.; et al. Differential diagnosis value of shear-wave elastography for superficial enlarged lymph nodes. *Front. Oncol.* **2022**, *12*, 908085. [CrossRef]
50. Wang, B.; Guo, Q.; Wang, J.Y.; et al. Ultrasound elastography for the evaluation of lymph nodes. *Front. Oncol.* **2021**, *11*, 714660. [CrossRef]
51. Chae, S.Y.; Jung, H.N.; Ryoo, I.; et al. Differentiating cervical metastatic lymphadenopathy and lymphoma by shear wave elastography. *Sci. Rep.* **2019**, *9*, 12396. [CrossRef]
52. Jung, W.; Chung, J.; Lee, J.; et al. Quantifying radiation-induced breast fibrosis by shear-wave elastography in patients with breast cancer: A 12-months-follow-up data of a prospective study. *Clin. Transl. Radiat. Oncol.* **2024**, *46*, 100773. [CrossRef]
53. Ogura, I.; Nakahara, K.; Sasaki, Y.; et al. Usefulness of shear wave elastography in the diagnosis of oral and maxillofacial diseases. *Imaging Sci. Dent.* **2018**, *48*, 161–165. [CrossRef]
54. Olchowy, C.; Grzech-Leśniak, K.; Hadzik, J.; et al. Monitoring of changes in masticatory muscle stiffness after gum chewing using shear wave elastography. *J. Clin. Med.* **2021**, *10*, 2480. [CrossRef]
55. Xue, F.; Wu, B.Z.; Zhang, R.; et al. The use of shear wave elastography to monitor changes in gingival elasticity associated with initial periodontal therapy in patients with advanced periodontitis: A prospective pilot study. *J. Dent. Sci.* **2023**, *18*, 1086–1093. [CrossRef]
56. Sathish, S.; Jain, A. The Sivan three-dimensional cone-beam computed tomography volumetric imaging protocol: A novel dual-mode rendering technique for integrated visualization of temporomandibular joint disc and osseous structures to evaluate temporomandibular joint disorders. *Oral Radiol.* **2026**, *42*, 148–161. [CrossRef]
57. Paluch, Ł.; Maj, P.; Pietruski, P.; et al. Shear wave elastography in the evaluation of temporomandibular joint disorders. *Ultrasound Med. Biol.* **2020**, *46*, 46–54. [CrossRef]
58. Öztürk, M.; Çalışkan, E.; Habibi, H.A. Shear wave elastography of temporomandibular joint disc and masseter muscle stiffness in healthy children and adolescents: A preliminary study. *Oral Radiol.* **2021**, *37*, 618–624. [CrossRef]
59. Olchowy, A.; Seweryn, P.; Olchowy, C.; et al. Assessment of the masseter stiffness during conservative therapy using shear wave elastography. *BMC Musculoskelet. Disord.* **2022**, *23*, 439. [CrossRef]
60. Chen, Y.J.; Lin, H.Y.; Chu, C.A.; et al. Assessing thickness and stiffness of superficial/deep masticatory muscles in orofacial pain: An ultrasound and shear wave elastography study. *Ann. Med.* **2023**, *55*, 2261116. [CrossRef]
61. Güven, F.; Akkuş, A.T.; Dinçkal Yanikoğlu, N.; et al. Shear wave elastography as a diagnostic method for bruxism. *Medicine* **2025**, *104*, e46183. [CrossRef]
62. Toker, C.; Marquetand, J.; Symmank, J.; et al. Shear wave elastography in bruxism—Not yet ready for clinical routine. *Diagnostics* **2023**, *13*, 276. [CrossRef]
63. McQueen, A.S.; Bhatia, K.S. Head and neck ultrasound: Technical advances, novel applications and the role of elastography. *Clin. Radiol.* **2018**, *73*, 81–93. [CrossRef]